

Transient statistics in stabilizing periodic orbits

R. Meucci, W. Gadowski,* M. Ciofini, and F. T. Arecchi[†]

Istituto Nazionale di Ottica, Firenze, Italy

(Received 16 May 1995; revised manuscript received 10 July 1995)

The statistics of chaotic and periodic transient time intervals preceding the stabilization of a given periodic orbit have been experimentally studied in a CO₂ laser with modulated losses, subjected to a small subharmonic perturbation. As predicted by the theory, an exponential tail has been found in the probability distribution of chaotic transients. Furthermore, a fine periodic structure in the distributions of the periodic transients, resulting from the interaction of the control signal and the local structure of the chaotic attractor, has been revealed.

PACS number(s): 05.45.+b, 42.50.Lc, 42.55.Lt

INTRODUCTION

The problem of controlling chaotic systems has been studied both theoretically and experimentally by many authors. An efficient method for achieving control was proposed by Ott, Grebogi, and Yorke [1]. Variations of this method have been successfully used to stabilize optical chaos [2] and for tracking steady states [3]. Alternative implementations for controlling chaos to periodic orbits are based (i) on the use of a continuous delayed feedback [4], (ii) on the introduction of small modulations of a control parameter [5,6], and (iii) on the knowledge of a prescribed goal dynamics [7]. Anyway, although the general processes characterizing different methods of control are understood, several interesting features, such as the transient approach to a stabilized orbit, have not been experimentally investigated.

In the present paper we report experiments on the transient dynamics which precedes the stabilization of a periodic orbit. In particular, we refer to a CO₂ laser where chaos has been obtained via periodic modulation (driving) of the cavity losses [8]. The stabilization of periodic orbits has been achieved with a parametric perturbation having relative amplitude of a few percent and frequencies in the ratios 1:2 and 1:4 with respect to the driving signal [6]. In order to obtain the transient time statistics, we have then applied a perturbation enveloped by a rectangular signal. We call this configuration "elementary," meaning that the perturbation is "open loop" (i.e., it does not enter a feedback loop) and it contains only the lowest subharmonic of the driving force.

Switching the perturbation on in a chaotic parameter range, the motion appears to be irregular and indistinguishable from the motion on the chaotic attractor for a certain time interval t_1 , before the stable orbit is approached [1,9]. First, we focused our attention on such a

chaotic transient. It has been theoretically proved that the length of the chaotic transient depends sensitively on the initial conditions. If one considers randomly distributed initial conditions, t_1 is expected to have an exponential probability distribution [1,9]. The analysis of our data on a CO₂ laser gives the first experimental evidence (to our knowledge) of this feature. The chaotic transient t_1 is usually followed by a regular oscillation converging with a monotonic behavior toward the stable orbit, with a characteristic time t_2 . The experimental probability distributions of the times t_2 show a periodic envelope which can be interpreted as due to the interaction of the control signal with the local periodic structure of the chaotic attractor.

The above classifications in terms of t_1 and t_2 presents some analogies with the results reported by Tel [10] in controlling transient chaos using the Ott, Grebogi, and Yorke (OGY) method [1]. In fact, whenever a system exhibits transient chaos, its phase space has an invariant set called a chaotic saddle or repellor, together with an attractor that is often periodic. As proved by Tel, it is possible to describe the escape from the repellor as separated from the decay into the target region.

EXPERIMENTAL SETUP AND RESULTS

The experimental setup has been described in detail in Ref. [6]. It consists of a single mode CO₂ laser with sinusoidal modulation of the cavity losses $\kappa(t)$, realized via an intracavity electro-optic modulator driven by a voltage signal $V(t)$,

$$\kappa(t) = \frac{c}{2L} \left[2T + (1-2T) \sin^2 \left[\frac{\pi V(t)}{V_\lambda} \right] \right],$$

$$V(t) = V_0 + V_1 A \sin(2\pi f_1 t),$$

where $L=2.0$ m is the cavity length, $T=0.10$ is the total transmission coefficient for a single pass, $V_\lambda=4240$ V is the half-wave voltage, $V_0=600$ V is a fixed bias voltage, $A=70$ is an amplification factor, and $f_1=100$ kHz is the fundamental driving frequency. In order to achieve stabilization on a given periodic orbit, a further amplitude

*Present address: Chemistry Department, University of Warsaw, Warsaw, Poland.

[†]Also at the Department of Physics, University of Florence, Florence, Italy.

modulation with frequency $f_2 = f_1/2$ is then applied to the voltage V_1 ,

$$V_1(t) = V_1[1 + \varepsilon \sin(2\pi f_2 t + \alpha)].$$

ε is the relative amplitude of the perturbation and α is the relative phase between the fundamental signal and the perturbation itself. As demonstrated in Ref. [6], a perturbation amplitude ε of a few percent is sufficient to stabilize different periodic orbits depending on the relative phase α .

For the particular purpose of this experiment the relative phase is fixed at a value which assures the best performance of control [6], and the perturbation signal is gated by a square wave triggered with the reference output of the master oscillator at 100 kHz (the response time of this circuit is less than 1 μ s). The laser signal and the gated signal have been stroboscopically recorded by a digital oscilloscope with an external clock of period $T = 10$ μ s corresponding to f_1 . These signals are shown in Fig. 1 for two different cases: (a) transient from chaotic attractor towards a stable orbit of period 2, with $V_1 = 1.35$ V, $\varepsilon = 0.070$, and $\alpha = \pi/2$; (b) transient from chaotic attractor towards a stable orbit of period 4, with $V_1 = 1.35$ V, $\varepsilon = 0.040$, and $\alpha = \pi/2$. When the control is activated, the trajectory initially evolves as in the free running case and, after the chaotic transient t_1 , it approaches the

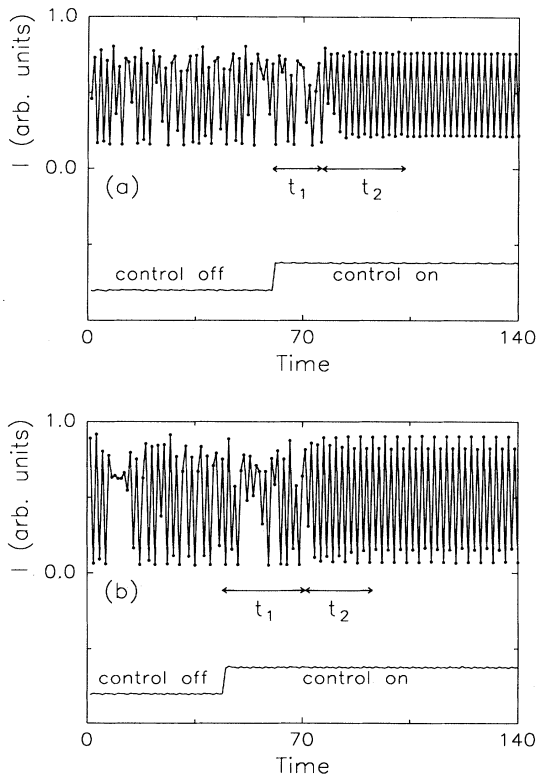


FIG. 1. Experimental stroboscopic recording of the laser intensity I during a transient to a stable orbit of period 2(a) and 4(b). t_1 denotes the duration of the chaotic transient, t_2 the decay to the selected stable orbit. (The horizontal scale is the time measured in periods since the sampling interval is 10 μ s.)

selected orbit of period 2 or 4 in a time interval t_2 .

The time interval $t = t_1 + t_2$ is measured from the moment of the control switch on to the moment at which the intensity levels of the stabilized signal [two levels in Fig. 1(a), four levels in Fig. 1(b)] reach a threshold of 95% of their asymptotic values. Morphologically, t_1 corresponds to erratic fluctuations, whereas during t_2 the signal displays a monotonic behavior (as shown in the figures) and the separation of the two behaviors is always marked by the appearance of a transient period-3 orbit.

The statistical distributions of t_1 and t_2 extracted from the complete time series corresponding to Fig. 1(b) (148 transients) are shown in Fig. 2. Similar results have been obtained from the data corresponding to Fig. 1(a). The distributions of the time intervals t_1 [Fig. 2(a)] have been fitted with an exponential law (solid line) having a time constant of 9.4 periods. The histogram of the time intervals t_2 is presented in Fig. 2(b). This figure clearly demonstrates the presence of a mechanism which modulates the probability distribution. This feature will be further discussed in the next section. Finally, according to the analysis of the data which reveals that t_1 and t_2 are completely uncorrelated, the distribution of $t = t_1 + t_2$ also presents an exponential tail [Fig. 2(c), decay time of 13.6 periods].

A complementary approach to characterize the transient toward a stable orbit can be introduced. Consider, for example, the case of Fig. 1(b) where a final period-4 orbit is reached. We can sample the signal with periodicity $4T$ and, identifying one of the four intensity levels, we can reconstruct the statistical distribution of the intensity at different times lying between the switch on and the switch off of the control. Figure 3 shows the time evolution of the first two moments of such a distribution, i.e., its average and standard deviation. The data reported in Fig. 3(a) can be successfully fitted with an exponential law which gives a time constant of 7.9 periods. Although this “transient intensity” statistical method seems easier to use, it presents the disadvantage of washing out all the fine structure details that are preserved by using “transient time” statistics.

NUMERICAL ANALYSIS AND INTERPRETATION

The above statistical methods have also been applied to data obtained from numerical simulations based on the four-level model (4LM) [6]. Such a model, including the coupling between the two resonant laser levels and their rotational manifolds, has been demonstrated to provide quantitative agreement with experiments on chaotic dynamics and controlling chaos. The 4LM consists of five differential equations for the laser intensity I , the populations N_2 and N_1 of the upper and lower lasing levels, and the global populations M_2 and M_1 of the two manifolds of rotational levels which are coupled by collisions with N_2 and N_1 :

$$\dot{I} = -\kappa I + G(N_2 - N_1)I,$$

$$\dot{N}_2 = -(z\gamma_R + \gamma_2)N_2 - G(N_2 - N_1)I + \gamma_R M_2 + \gamma_2 P,$$

$$\dot{N}_1 = -(z\gamma_R + \gamma_1)N_1 + G(N_2 - N_1)I + \gamma_R M_1,$$

$$\dot{M}_2 = -(\gamma_R + \gamma_2)M_2 + z\gamma_R N_2 + z\gamma_2 P,$$

$$\dot{M}_1 = -(\gamma_R + \gamma_1)M_1 + z\gamma_R N_1,$$

where κ is the intensity decay rate, $\gamma_R = 7.0 \times 10^5 \text{ s}^{-1}$ is the relaxation rate between the lasing states and the associated rotational manifolds (the enhancement factor $z = 10$ represents the number of sublevels considered in each manifold), and $\gamma_1 = 8.0 \times 10^4 \text{ s}^{-1}$ and $\gamma_2 = 1.0 \times 10^4 \text{ s}^{-1}$ are the relaxation rates of the vibrational states.

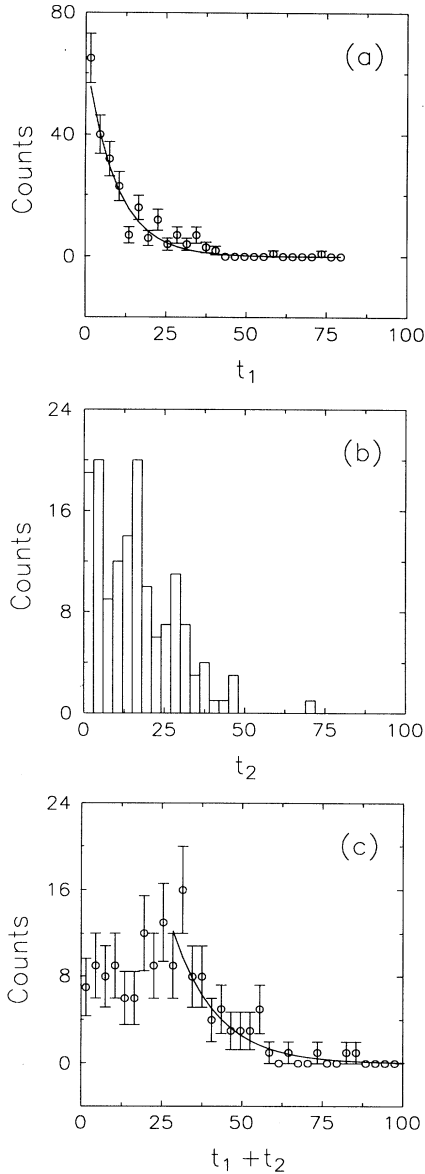


FIG. 2. Statistical analysis for the data corresponding to Fig. 1(b) (horizontal scale as in Fig. 1). (a) Probability distribution of t_1 ; the solid line represents the exponential fit (the error bars are estimated as the square root of the number of counts in each channel). (b) Histogram of the time intervals t_2 ; the width of each bar is three periods. (c) Probability distribution of $t = t_1 + t_2$ [error bars as in Fig. 2(a)]; the solid line represents an exponential fit of the tail of the distribution.

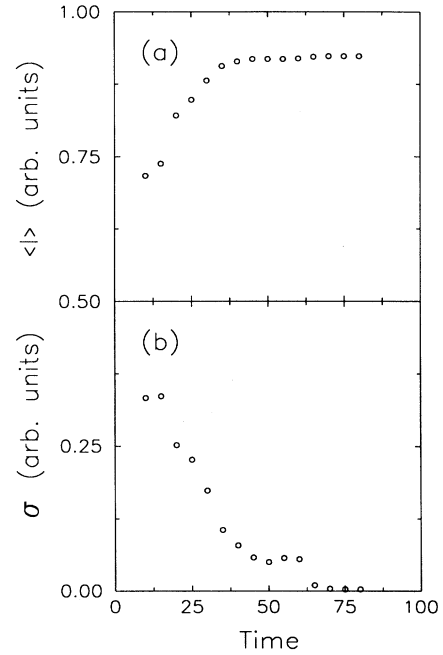


FIG. 3. Amplitude statistics of the data of Fig. 1(b); sampling the signal every $40 \mu\text{s}$ we have selected the points corresponding to the upper intensity level of the period-4 stable attractor. (a) Average intensity and (b) standard deviation, with horizontal scale as in Fig. 1.

Moreover, $G = 6.2 \times 10^{-8} \text{ s}^{-1}$ is the field-matter coupling constant, while the adimensional parameter $P = 6.35 \times 10^{14}$ represents the pump (the numerical values of the parameters are chosen by following Ref. [6]).

As in the experiment, we focused our interest on the stabilization of a given periodic orbit. Figure 4 shows a stroboscopic recording of the laser intensity during a transient from a chaotic to a period-4 stable orbit ($V_1 = 1.40 \text{ V}$, $\varepsilon = 0.073$, $\alpha = \pi/2$). Also in this case, the total time duration necessary for stabilization has been separated into two parts, a chaotic transient of duration

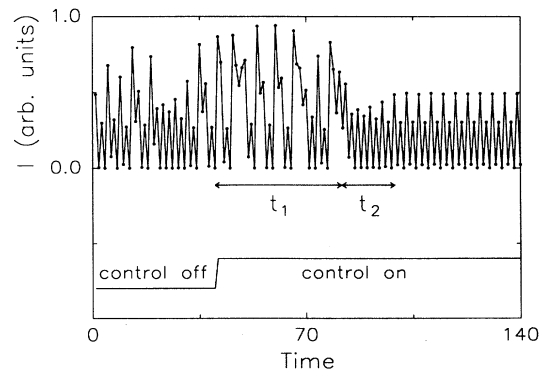


FIG. 4. Numerical simulation of the transition from a chaotic to a period-4 stable orbit showing the chaotic transient t_1 and the regular decay t_2 (horizontal scale as in Fig. 1).

t_1 and a decay of duration t_2 . The characteristic exponential decays shown in Figs. 2(a) and 2(c) are well reproduced in the numerical distributions of t_1 [Fig. 5(a), time constant 9.6 periods] and of $t = t_1 + t_2$ [Fig. 5(c), time constant 12.6 periods], respectively. Regarding the Lyapunov exponents, we note that the transition from chaotic to stabilized period-4 orbit is characterized by a change of the leading exponent λ_1 from 1.96×10^4 to -4.26×10^3 Hz. The inverse of this last value (≈ 23.5 periods) is comparable with the above evaluated decay times. As regards the periodicity in the distribution of t_2 , Fig. 5(b) clearly demonstrates the presence of this feature. Here we have chosen a bar width of two periods in order to emphasize the periodicity. This periodicity, however, remains evident even if the distribution is calculated after

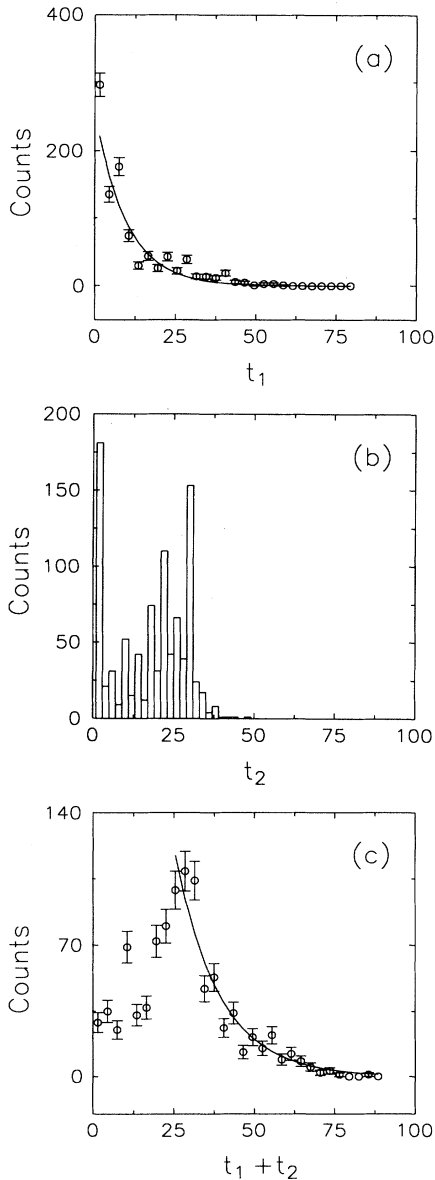


FIG. 5. Time statistics as in Fig. 2 performed over the data corresponding to Fig. 4 (with 960 transients).

adding a random number between 0 and 2 to each value of t_2 . This confirms that this feature is not an artifact due to our choice of the bar width. It is also interesting to observe that, due to the absence of noise, the numerical experiment reveals a finer structure than that shown in Fig. 2(b).

A perturbative approach can provide a simple interpretation of the modulation in the probability distribution of t_2 . Let us first consider a period- N solution of a modulated system in the form

$$y \sim e^{i2\pi t/NT} + \text{c.c.} = x^{1/N} + \text{c.c.},$$

where $x = \exp[i2\pi t/T]$. $F = x + \text{c.c.}$ represents the unperturbed driving signal. In the case of small amplitude modulation with period $2T$, the perturbed driving signal $F + \Delta F$ can be expressed as

$$F + \Delta F = [1 + \varepsilon(x^{1/2} + \text{c.c.})](x + \text{c.c.}),$$

$$\Delta F = \varepsilon(x + \text{c.c.})(x^{1/2} + \text{c.c.}).$$

The perturbed solution y_1 can be expanded according to

$$y_1 = y + \left[\frac{\partial y}{\partial x} \right] \left[\frac{\partial x}{\partial F} \right] \Delta F.$$

Taking into account the approximated expression for ΔF and after some algebra, it is easy to verify that the correction in y_1 contains terms with the following fractional ratios r_j ($j = 1-4$) of the fundamental frequency:

$$r_1 = \frac{1-N}{N} \pm \frac{3}{2}, \quad r_2 = \frac{1-N}{N} \pm \frac{1}{2},$$

$$r_3 = -\frac{1+N}{N} \pm \frac{3}{2}, \quad r_4 = -\frac{1+N}{N} \pm \frac{1}{2}.$$

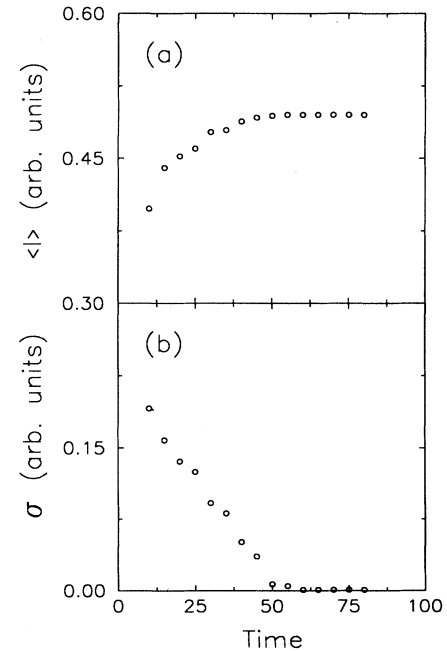


FIG. 6. Amplitude statistics as in Fig. 3 performed over the data corresponding to Fig. 4.

For the particular case corresponding to $N=4$ the lowest value of r_j is $\frac{1}{4}$. Considering this result, we suggest that the periodicity of the observed echolike modulation is related to integer multiples of r_j/T , that is, to the interaction between the periodicity of the perturbation and that of the trajectory.

Figure 6 reports the results obtained by applying "transient intensity" statistics [the time constant for the data of Fig. 6(a) is 8.0 periods].

CONCLUSIONS

To conclude, we have analyzed the transient statistics in controlling chaos in a CO₂ laser with modulated losses subjected to a gated control perturbation at the lowest subharmonic of the fundamental driving force. The statistics of the chaotic transients t_1 presents an exponential tail as predicted by the theory. Moreover, the pertur-

bation, interacting with the local structure of the attractor, determines a periodic structure in the distribution of the time t_2 which governs the decay toward the stabilized orbit. Such a structure can be easily recognized by using passage time statistics. In contrast, the complementary approach, namely, the intensity statistics, does not give evidence of this effect. Numerical tests both provide a satisfactory agreement with the experimental distributions and confirm the differences between the two statistical approaches.

ACKNOWLEDGMENTS

This work was partly supported by the E.C. Contract No. CHRX-CT93-0107. One of the authors (W.G.) has been partly supported by KBN Grant No. 2P03B 158 08 (University of Warsaw, Poland).

-
- [1] E. Ott, C. Grebogi, and J. A. Yorke, *Phys. Rev. Lett.* **64**, 1196 (1990). See also the review paper T. Shinbrot, C. Grebogi, E. Ott, and J. A. Yorke, *Nature* **363**, 411 (1993).
 - [2] R. Roy, T. W. Murphy, T. D. Maier, Z. Gills, and E. R. Hunt, *Phys. Rev. Lett.* **68**, 1259 (1992).
 - [3] I. B. Schwartz and I. Triandaf, *Phys. Rev. A* **46**, 7439 (1992); T. L. Carroll, I. Triandaf, I. B. Schwartz, and L. Pecora, *ibid.* **46**, 6189 (1992); Z. Gills, C. Iwata, R. Roy, I. B. Schwartz, and I. Triandaf, *Phys. Rev. Lett.* **69**, 3169 (1992).
 - [4] K. Pyragas, *Phys. Lett. A* **170**, 421 (1992); S. Bielawski, D. Derozier, and P. Glorieux, *Phys. Rev. E* **49**, R971 (1994); J. E. S. Socolar, D. W. Sukow, and D. J. Gauthier, *ibid.* **50**, 3245 (1994).
 - [5] R. Lima and M. Pettini, *Phys. Rev. A* **41**, 726 (1991); Y. Braiman and I. Goldhirsch, *Phys. Rev. Lett.* **66**, 2545 (1991); R. Chacón and J. Diaz Berjarano, *ibid.* **71**, 3103 (1993); Y. Liu and J. R. Rios Leite, *Phys. Lett. A* **185**, 35 (1994); Y. Liu, N. Kikuchi, and J. Ohtsubo, *Phys. Rev. E* (to be published); T. Tsukamoto, M. Tachikawa, and T. Sugawara, *Phys. Rev. A* (to be published).
 - [6] R. Meucci, W. Gadomski, M. Ciofini, and F. T. Arecchi, *Phys. Rev. E* **49**, R2528 (1994).
 - [7] B. B. Plapp and A. Hübler, *Phys. Rev. Lett.* **65**, 2302 (1990).
 - [8] F. T. Arecchi, R. Meucci, G. P. Puccioni, and J. R. Tredicce, *Phys. Rev. Lett.* **49**, 1217 (1982); A. Poggi, W. Gadomski, J. R. Tredicce, and F. T. Arecchi, *ibid.* **55**, 339 (1985); D. Dangoisse, P. Glorieux, and D. Hennequin, *ibid.* **57**, 2657 (1986); I. B. Schwartz, *ibid.* **60**, 1359 (1988).
 - [9] C. Grebogi, E. Ott, and J. A. Yorke, *Physica D* **7**, 181 (1983); *Phys. Rev. Lett.* **57**, 1284 (1986).
 - [10] T. Tel, *J. Phys. A* **24**, L1359 (1991).